INVESTIGATION ON THE INTERACTION ANALYSIS OF BEAM-NONLINEAR ISOLATOR WITH LOW AND HIGH STIFFNESS SUPPORT

K. K. Turahim[1*], K. Djidjeli[2], J. T. Xing[3]

[1,2,3]Faculty of Engineering and Physical Science, University of Southampton, University Rd, Southampton SO17 1BJ, England.

Article History: Received 9.7.2019; Revised 3.11.2019; Accepted 2.12.2019

ABSTRACT

This paper presents the study of the interaction between a beam and a nonlinear isolator for low and high supporting stiffness. The system consists of an elastic beam- like structure and a geometrically nonlinear isolation system in which a horizontal degree provides a physical approach for realising the required horizontal force. The generalised dynamic equations of the system are derived and the modal summation method is used to analyse the beam. The dynamic interaction mechanism between the nonlinear isolation system and the elastic structure is revealed. The beam- nonlinear isolator design for low stiffness support and high stiffness support is discussed. It is found that the beam provides additional mass, stiffness and force to the nonlinear vibration isolator and the requirement to perform ground vibration test whereby the rigid mode of the beam must be less than one third of the first elastic natural frequency of the free-free beam has been satisfied. The condition to achieve high stiffness support has also been satisfied. Nonlinear dynamical behaviour of the beam-nonlinear isolator indicates that period doubling bifurcation occurs when the excitation force is 1 and excitation frequency is 0.5Hz. Poincare' maps reveals that the system form closed loops and no chaotic behaviour is observed. Perfomance analysis in terms of force transmissibility of the nonlinear isolator shows that the nonlinear isolator performs better than a linear isolator and also performs better than a hardening HSLDS mount.

KEYWORDS*: Beam, Nonlinear isolator; interactions; bifurcation; Poincare'*

*Corresponding Email: khairiah.turahim@gmail.com

1.0 INTRODUCTION

Vibration isolation systems with particular low or high suspension frequencies are of great importance in scientific and industrial fields. For ground vibration tests (GVT) of very large civil aircrafts, the suspension frequency required is less than 1/3 of the system's fundamental frequency (Green, 1945). The aim of GVT is to simulate an aircraft in a free-free state on the ground. For large thin-wing aircraft with fundamental frequencies below 1 Hz, some further development in methods of support is necessary. An application that requires a high suspension frequency can be found in laboratory vibration tests, whereby a rigid boundary condition of the foundation is often assumed, thus the dynamic supporting stiffness is required to be very high up to infinity (Wagg & Nield, 2010). Due to the limitation of traditional linear passive isolation units, it is hard to achieve these particular low and high suspension frequency. According to Inman (2007) , passive isolation units experience an issue of static deflection whereby it can perform very well when the systems natural frequency is decreased, which will increase its isolation frequency bandwidth. Unfortunately, a low natural frequency, which means having a low supporting stiffness, will result in a large static deflection which is undesirable. Currently there is a growing interest in the study of nonlinear isolators due to the benefits of nonlinearity and the fact that many practical isolators exhibit nonlinear behaviour (Kovacic et al. 2008). Linear passive vibration isolators are only effective if the excitation frequency is larger than $\sqrt{2}$ times the natural frequency. The lower the static stiffness of a system and hence the lower the natural frequency, the wider the isolation region. However, a low static stiffness causes a large static deflection. This can be overcome by adding oblique springs to obtain a high static stiffness, small static displacement, small dynamic stiffness and hence low natural frequency (Rivin, 2003). Practical isolation units have to be connected on to the supported structures, hence the structure vibration behaviour and the isolation dynamic characteristics will affect each other. Therefore, the practical system is a structure-isolation unit interaction system. To design an accurate practical isolation system, the interaction analysis is necessary. This research will consider the structure and isolation unit as an integrated interaction system to investigate its vibration behaviours using a numerical approach.

2.0 BEAM-NONLINEAR ISOLATOR GENERAL MODEL

The integrated interaction system consists of an elastic structure which is supported by a nonlinear isolation unit as shown in Figure 1. The structure is considered as a uniform elastic free-free beam subject to two harmonic forces $F_0 \cos \Omega_0 t$ applied symmetrically at point ξ_0 under the beam coordinate system O–ξY fixed at the middle point O of the beam. There is a lumped mass $2M$ connected at point O by a rigid rod of which the mass is included into $2M$. The beam is of span length $2S$, mass density ρ per unit length and bending stiffness Ψ=EI. Since the beam is elastic, its deflection $Y(\xi,t)$ is a function of beam material point ξ and time t. The lumped mass $2M$ is supported by a generalised nonlinear isolation system symmetrical to the vertical axis o–y, and therefore it moves in the y direction only. The two linear inclined massless springs of stiffness k and non-stretched length l are connected to the mass $2M$ with their other two ends being respectively connected to the two carts A and B of mass m allowing horizontal motions. There are two horizontal massless springs of stiffness K_1 and non-stretched length L_1 as well as two dampers of damping coefficient C_1 connected to carts A and B, respectively. Along the symmetrical axis o–y, a spring-damper set consisting of a spring of stiffness $2K$ and non-stretched length L and a damper of damping coefficient $2C$ is connected to the mass $2M$. The coordinate x can identify the positions of the two carts.

The model shown in Figure 1 is a generalised model of structure-nonlinear suspension interaction system. The arranged elements in this model are to realise practical designs for engineering applications. The horizontal spring-damper unit (K_1, C_1) aims to provide a means to realise the two horizontal forces added at the two carts to adjust the vertical dynamic stiffness of the total system. A suitable adjustment of the initial length L_1 of the spring K_1 results in a pull or push force applied at the two carts A and B, which increases or decreases the vertical supporting stiffness of the system, respectively. The vertical spring-damper unit (K, C) supports the static weight of the mass $2M$ and the structure. The two spring-damper units (k, c) are the main elements with geometric nonlinear characteristics to adjust the dynamic supporting stiffness. The dampers in the system provide the adjusted parameters for the stability requirement of the system. Based on this generalised model, several simplified models (Platus, 1992), (Cao et al., 2008a,2008b), (Liu et al., 2012) can be obtained by introducing additional conditions or reducing some elements.

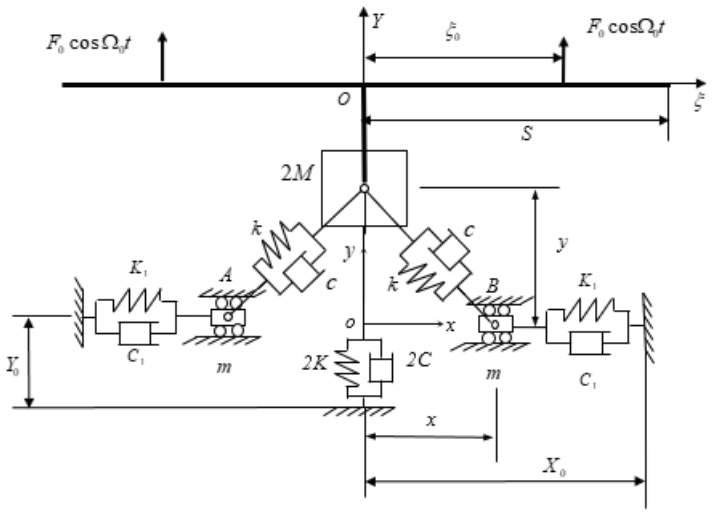

Figure 1 An integrated interaction system consisting of an elastic beam and a generalised nonlinear isolation unit (Xing, 2017)

2.1 Governing Equations of Integrated Interaction System

Considering the symmetry of the system in Figure 1, the right-half part of the system was investigated to derive the governing equations. It would be convenient to choose origin o of coordinate system $o-xy$ and origin O of beam coordinate system $O-\xi Y$ respectively located at their corresponding positions in a static equilibrium state when the mass $2M$ and the two inclined springs k are on the horizontal axis $o-x$ with mass m at x_o. To realise this, we can choose a suitable extension $\Delta=Y_0-L$ of the vertical spring K by investigating the static equilibrium of the system subject to the gravity only, i.e.

$$\begin{aligned} K\Delta &= -g(M+\rho S), & \Delta &= -g(M+\rho S)/K, \\ (K_1+k)x_0 - kl &= K_1\Delta_1, & \Delta_1 &= X_0 - L_1 \end{aligned} \tag{1}$$

2.1.1 *Dynamic equilibrium equation and boundary conditions of beam structure*

The dynamic equilibrium equation of the beam is

$$\Psi \frac{\partial^4 Y}{\partial \xi^4} + \rho \frac{\partial^2 Y}{\partial t^2} = \delta(\xi - \xi_0) F_0 \cos \Omega_0 t; \tag{2}$$

and the boundary conditions are: $Y'' = 0 = Y''', \xi = S; Y' = 0, \Psi Y'' = f_{bs}, \xi = 0$

Here, f_{bs} represents a dynamic shearing force acted on the beam section $\xi = 0$ by the rigid rod, $\delta()$denotes delta function.

The beam is considered as a linear elastic structure, so that its motion can be represented in its mode space using a mode superposition method (Thomson, 1996). In engineering, there are many nonlinear systems consisting of linear substructures connected by nonlinear connectors. For this type of nonlinear system, the mode superposition approach provides a very effective numerical model to study the motions of linear substructures (Xing & Price, 1991).

The deflection Y(ξ,t) of the beam is represented by a mode summation form

$$Y(\xi,t) = \boldsymbol{Y}(\xi)\boldsymbol{\Phi}(t), \tag{3}$$

where

$$\begin{aligned} &\boldsymbol{Y} = [Y_1 \quad Y_2 \quad \cdots \quad Y_N], \quad \boldsymbol{\Phi} = [\varphi_1 \quad \varphi_2 \quad \cdots \quad \varphi_N]^T, \\ &Y_n(\xi) = \frac{1}{2}\{\frac{cosh(\lambda_n\xi/S)}{cosh\,\lambda_n} + \frac{cos(\lambda_n\xi/S)}{cos\,\lambda_n}\}, \\ &tan\,\lambda_n + tanh\,\lambda_n = 0, \qquad n = 1,2,3,\cdots \end{aligned} \tag{4}$$

based on the non-dimensional symmetrical mode functions Y_n (ξ),(n=1,2,...,N), of the uniform free-free beam. Here, N denotes a number of the retained mode functions $Y_n(\xi)$ and φ_n represents a generalised coordinate corresponding to mode n, which has a length dimension. These mode functions satisfy the following orthogonal relationships,

$$\int_0^S Y_n'' EIY_j''\, d\xi = \begin{cases} 0, & n \neq j, \\ K_{nn}, & n = j, \end{cases}$$

$$\int_0^S Y_n \rho Y_j\, d\xi = \begin{cases} 0, & n \neq j, \\ M_{nn}, & n = j, \end{cases}$$

$$\begin{aligned} M_{nn} &= \begin{cases} \rho S, & n = 1, \\ \rho S/4, & n \neq 1, \end{cases} \\ K_{nn} &= \begin{cases} 0, & n = 1, \\ \dfrac{\lambda_n^4 \Psi}{4S^3}, & n \neq 1, \end{cases} \\ \hat{\Omega}_n &= \sqrt{K_{nn}/M_{nn}} = \frac{\lambda_n^2}{S^2}\sqrt{\frac{\Psi}{\rho}} \end{aligned} \tag{5}$$

The sub-index n indicates the mode number of the free-free beam, $\hat{\Omega}_n$, K_n and M_n represent the n-th natural frequency, generalised stiffness and mass, respectively. For the free-free beam, its first mode is a rigid mode with frequency $\hat{\Omega}_1 = 0$ and mode function $Y_1 = 1$.

Substituting Equation (3) into Equation (2) and using the orthogonal relationships (5), we obtain the following mode equation describing the beam motion

$$\begin{aligned} &\boldsymbol{m}\ddot{\boldsymbol{\Phi}} + \boldsymbol{k}\boldsymbol{\Phi} = \boldsymbol{Y}^T(0) f_{bs} + \boldsymbol{Y}^T(\xi_0) F_0 \cos \Omega_0 t, \\ &\boldsymbol{m} = \mathrm{diag}(M_{nn}), \qquad \boldsymbol{k} = \mathrm{diag}(K_{nn}), \qquad \boldsymbol{\Lambda}^2 = \mathrm{diag}(\hat{\Omega}_n^2) \end{aligned} \tag{6}$$

2.1.2 *Dynamic equilibrium equations of the nonlinear supporting unit*

The dynamic equilibrium equation of the nonlinear supporting unit is

$$\boldsymbol{M}\ddot{\boldsymbol{x}} + (\boldsymbol{C} + \boldsymbol{C}_c)\dot{\boldsymbol{x}} + (\boldsymbol{K} + \boldsymbol{K}_k)\boldsymbol{x} = \begin{bmatrix} K_1 \Delta_1 \\ f_{sb} \end{bmatrix}, \tag{7}$$

where

$$\begin{aligned} &\boldsymbol{M} = \begin{bmatrix} m & 0 \\ 0 & M \end{bmatrix}, \quad \boldsymbol{C} = \begin{bmatrix} C_1 & 0 \\ 0 & C \end{bmatrix}, \quad \boldsymbol{C}_c = \frac{c}{\mu^2}\boldsymbol{x}\boldsymbol{x}^T, \\ &\qquad \boldsymbol{K} = \begin{bmatrix} K_1 + k & 0 \\ 0 & K + k \end{bmatrix}, \\ &\boldsymbol{K}_k = -\frac{kl}{\mu}\boldsymbol{I}, \quad \boldsymbol{I} = \begin{bmatrix} 1 & 0 \\ 0 & 1 \end{bmatrix}, \quad \boldsymbol{x} = [x \quad y]^T, \quad \Delta_1 = X_0 - L_1, \\ &\qquad \mu = \sqrt{x^2 + y^2} \end{aligned} \tag{8}$$

Here, Δ_1 represents the static extension of horizontal spring K_1 in the static state defined by Equation (1). The force f_{sb} denotes the reaction force from the beam to the lumped mass $2M$. The nonlinearity is given by μ which describes the oblique position of the spring, k and damper, c.

On the interaction section $\xi = 0$ between the beam and the nonlinear suspension unit, a dynamic equilibrium condition and a geometrical constraint condition are required, i.e.

Equilibrium: $$f_{bs} + f_{sb} = 0, \qquad -f_{bs} = f_{sb} = f, \tag{9}$$

Geometrical constraint: $$Y(0,t) = y(t), \tag{10}$$

which, when Equation (3) is used, is written in the mode form

$$\boldsymbol{Y}_0\boldsymbol{\Phi} = y, \qquad \boldsymbol{Y}_0 = \boldsymbol{Y}(0) \tag{11}$$

Equation (1) to (11) give the governing equations describing the dynamics of the integrated interaction system.

2.1.3 Non- dimensional dynamic equations

To derive the non-dimensional equations of the system, the following non-dimensional parameters are introduced

$$\bar{x} = \frac{x}{l},\ \bar{x}_0 = \frac{x_0}{l},\ \bar{y} = \frac{y}{l},\ \bar{\Delta}_1 = \frac{\Delta_1}{l},\ \bar{\Delta} = \frac{\Delta}{l},\ \bar{t} = \Omega_0 t,\ \bar{Y} = \frac{Y}{l},\ \bar{\xi} = \frac{\xi}{l},\ \bar{S} = \frac{S}{l},$$

$$\omega = \sqrt{(k+K_1)/m},\ \bar{\omega} = \frac{\Omega_0}{\omega},\ E_1 = \frac{C_1}{2m\omega},\ \bar{m} = \frac{m}{M},\ \bar{\rho} = \frac{\rho l}{M}, \omega = \sqrt{\omega_k^2 + \omega_1^2},$$

$$\omega_k = \sqrt{\frac{k}{m}},\ \omega_1 = \sqrt{\frac{K_1}{m}},\ \bar{\omega}_k = \frac{\omega_k}{\Omega_0},\ \bar{\omega}_1 = \frac{\omega_1}{\Omega_0},\ \widetilde{\omega}_k = \frac{\omega_k}{\omega},\ \widetilde{\omega}_1 = \frac{\omega_1}{\omega},$$

$$\widetilde{K}_1 = \frac{K_1}{k+K_1},\ \bar{K}_1 = \bar{m}\widetilde{K}_1\bar{\omega}^2 = \frac{K_1\Omega_0^2}{M\omega^4},\ \bar{k} = \tilde{k}_K\bar{\Omega}^2 = \bar{m}\tilde{k}_1\bar{\omega}^2 = k\Omega_0^2/(M\omega^4),$$

$$\tilde{k}_1 = \frac{k}{k+K_1}, \tilde{k}_K = \frac{k}{k+K},\ \widetilde{c}_1 = \frac{c}{C_1},\ \widetilde{c}_K = \frac{c}{C},\ \bar{\varepsilon} = \tilde{c}_K E\bar{\Omega} = \bar{m}\tilde{c}_1 E_1\bar{\omega} = \frac{c\Omega_0}{2M\omega^2}, \tag{12}$$

$$\Omega = \sqrt{(k+K)/M},\ \bar{\Omega} = \frac{\Omega_0}{\Omega}, E = \frac{C}{2M\Omega}, \bar{g} = \frac{g}{\Omega_0^2 l}, \Omega = \sqrt{\Omega_k^2 + \Omega_K^2},$$

$$\Omega_k = \sqrt{k/M},\ \Omega_K = \sqrt{K/M},\ \bar{\Omega}_k = \frac{\Omega_k}{\Omega_0},\ \bar{\Omega}_K = \frac{\Omega_K}{\Omega_0},\ \widetilde{\Omega}_k = \frac{\Omega_k}{\Omega},\ \widetilde{\Omega}_K = \Omega_K/\Omega,$$

$$\bar{F}_0 = \frac{F_0}{M\Omega^2 l},\ \bar{f}_1 = \bar{K}_1\bar{\Delta}_1,\ \bar{f} = \frac{f_{sb}}{M\Omega^2 l},\ \bar{\boldsymbol{m}} = \frac{\boldsymbol{m}}{M},\ \bar{\boldsymbol{\Phi}} = \frac{\boldsymbol{\Phi}}{l}, \bar{\boldsymbol{\Lambda}}^2 = \boldsymbol{\Lambda}^2/\Omega_0^2.$$

The dynamic equilibrium equation and boundary conditions of beam structure are

$$\bar{\boldsymbol{m}}\ddot{\bar{\boldsymbol{\Phi}}} + \bar{\boldsymbol{m}}\bar{\boldsymbol{\Lambda}}^2\bar{\boldsymbol{\Phi}} = \boldsymbol{R}\bar{\boldsymbol{f}} + \bar{\boldsymbol{F}}_0, \tag{13}$$

where $\boldsymbol{R} = [\boldsymbol{0} \quad -\boldsymbol{Y}_0^T], \bar{\boldsymbol{F}}_0 = \boldsymbol{Y}_F^T\bar{F}_0\ cos\ t\ , \boldsymbol{Y}_F = \boldsymbol{Y}(\xi_0), \boldsymbol{Y}_0\bar{\boldsymbol{\Phi}} = \bar{y}$

The dynamic equilibrium equation of the nonlinear supporting unit is

$$\bar{\boldsymbol{M}}\ddot{\boldsymbol{q}} + 2[\bar{\boldsymbol{M}}\bar{\boldsymbol{\omega}}\boldsymbol{E} + \boldsymbol{\varepsilon}(\boldsymbol{q})]\dot{\boldsymbol{q}} + [\bar{\boldsymbol{M}}\bar{\boldsymbol{\omega}}^2 + \boldsymbol{k}(\boldsymbol{q}) + \boldsymbol{k}_1(\boldsymbol{q})]\boldsymbol{q} = \bar{\boldsymbol{f}}, \tag{14}$$

where

$$\bar{\boldsymbol{M}} = \begin{bmatrix} \bar{m} & 0 \\ 0 & 1 \end{bmatrix}, \bar{\boldsymbol{\omega}} = \begin{bmatrix} \bar{\omega} & 0 \\ 0 & \bar{\Omega} \end{bmatrix}, \boldsymbol{E} = \begin{bmatrix} E_1 & 0 \\ 0 & E \end{bmatrix}, \boldsymbol{I} = \begin{bmatrix} 1 & 0 \\ 0 & 1 \end{bmatrix}, \boldsymbol{I}_1 = \begin{bmatrix} 1 & 0 \\ 0 & 0 \end{bmatrix}, \tag{15}$$

$$\boldsymbol{\varepsilon}(\boldsymbol{q}) = \frac{\bar{\varepsilon}}{\bar{\mu}^2}\boldsymbol{q}\boldsymbol{q}^T, \boldsymbol{k}(\boldsymbol{q}) = -\frac{\bar{k}}{\bar{\mu}}\boldsymbol{I}, \bar{\boldsymbol{f}} = \begin{bmatrix} 0 \\ \bar{f} \end{bmatrix}, \boldsymbol{k}_1(\boldsymbol{q}) = -\frac{\bar{f}_1}{q_1}\boldsymbol{I}_1, \bar{\mu} = \sqrt{\boldsymbol{q}^T\boldsymbol{q}}$$

Here, $\boldsymbol{\varepsilon}(\boldsymbol{q})$ and $\boldsymbol{k}(\boldsymbol{q})$ represent a nonlinear damping matrix and a nonlinear stiffness matrix of the system, respectively.

2.1.4 Integrated coupling matrix equation

Combining Equation (13) and (14), the integrated coupling equation of the system in matrix form is obtained

$$\hat{\boldsymbol{M}}\ddot{\boldsymbol{Q}} + (\hat{\boldsymbol{C}}^L + \hat{\boldsymbol{C}}^N)\dot{\boldsymbol{Q}} + (\hat{\boldsymbol{K}}^L + \hat{\boldsymbol{K}}^N)\boldsymbol{Q} = \hat{\boldsymbol{F}}_0 \tag{16}$$

where

$$\boldsymbol{Q} = \begin{bmatrix} q_1 \\ \bar{\boldsymbol{\Phi}} \end{bmatrix}, \boldsymbol{q} = \boldsymbol{T}\boldsymbol{Q}, \hat{\boldsymbol{M}} = \begin{bmatrix} \bar{m} & \boldsymbol{0}^T \\ \boldsymbol{0} & \bar{\boldsymbol{Y}} + \bar{\boldsymbol{m}} \end{bmatrix}, \boldsymbol{T} = \begin{bmatrix} 1 & 0 \\ \boldsymbol{0} & \boldsymbol{Y}_0 \end{bmatrix}, \hat{\boldsymbol{F}}_0 = \begin{bmatrix} 0 \\ \bar{\boldsymbol{F}}_0 \end{bmatrix},$$
$$\hat{\boldsymbol{C}}^N = 2\boldsymbol{T}^T\boldsymbol{\varepsilon}(\boldsymbol{q})\boldsymbol{T}, \hat{\boldsymbol{C}}^L = 2\boldsymbol{T}^T\bar{\boldsymbol{M}}\bar{\boldsymbol{\omega}}\boldsymbol{E}\boldsymbol{T} \tag{17}$$
$$\hat{\boldsymbol{K}}^L = \{\mathrm{diag}(0, \bar{\mathbf{m}}\bar{\boldsymbol{\Lambda}}^2) + \boldsymbol{T}^T\bar{\boldsymbol{M}}\bar{\boldsymbol{\omega}}^2\boldsymbol{T}\}, \hat{\boldsymbol{K}}^N = \boldsymbol{T}^T[\boldsymbol{k}(\boldsymbol{q}) + \boldsymbol{k}_1(\boldsymbol{q})]\boldsymbol{T}$$

The total degree of freedom of this system is 1+N where N is the mode number chosen to describe the beam motion. Equation (16) can be rewritten in the state space form

$$\begin{cases} \dot{\boldsymbol{Q}} = \boldsymbol{P} \\ \dot{\boldsymbol{P}} = \hat{\boldsymbol{M}}^{-1}\{\hat{\boldsymbol{F}}_0 - (\hat{\boldsymbol{C}}^L + \hat{\boldsymbol{C}}^N)\boldsymbol{P} - (\hat{\boldsymbol{K}}^L + \hat{\boldsymbol{K}}^N)\boldsymbol{Q}\} \end{cases} \tag{18}$$

Here, the super-indices "L" and "N" identify the linear parts and nonlinear parts of the matrices, respectively. The nonlinearity is given by by $\boldsymbol{\varepsilon}(\boldsymbol{q})$ and $\boldsymbol{k}(\boldsymbol{q})$ which represents a nonlinear damping matrix and a nonlinear stiffness matrix

as shown in Equation (14) and Equation (15). The coupling matrix in Equation (16) describes the dynamics of the integrated interaction system. Based on this set of equations, we can investigate the coupling mechanism between the elastic beam and the nonlinear suspension unit.

2.2 Interaction Analysis

2.2.1 Equation governing the influence of beam motions on nonlinear suspension system

From Equation (13), it follows that

$$\ddot{\bar{\boldsymbol{\Phi}}} + \bar{\boldsymbol{\Lambda}}^2\bar{\boldsymbol{\Phi}} = \bar{\boldsymbol{m}}^{-1}\boldsymbol{R}\bar{\boldsymbol{f}} + \bar{\boldsymbol{m}}^{-1}\bar{\boldsymbol{F}}_0, \quad \boldsymbol{R} = [\boldsymbol{0} \quad -\boldsymbol{Y}_0^T], \tag{19}$$

which, when pre-multiplied by $\boldsymbol{Y}_0$, gives

$$\begin{aligned}\boldsymbol{Y}_0\ddot{\bar{\boldsymbol{\Phi}}} + \boldsymbol{Y}_0\bar{\boldsymbol{\Lambda}}^2\bar{\boldsymbol{\Phi}} &= \boldsymbol{Y}_0\bar{\boldsymbol{m}}^{-1}\boldsymbol{R}\bar{\boldsymbol{f}} + \boldsymbol{Y}_0\bar{\boldsymbol{m}}^{-1}\bar{\boldsymbol{F}}_0 \\ &= -m_b^{-1}\bar{f} + \boldsymbol{Y}_0\bar{\boldsymbol{m}}^{-1}\bar{\boldsymbol{F}}_0, \qquad m_b^{-1} \\ &= \boldsymbol{Y}_0\bar{\boldsymbol{m}}^{-1}\boldsymbol{Y}_0^T\end{aligned} \tag{20}$$

Since

$$m_b^{-1} = \boldsymbol{Y}_0\bar{\boldsymbol{m}}^{-1}\boldsymbol{Y}_0^T = \sum_{n=1}^{N}\bar{M}_{nn}^{-1}\,Y_{n0}^2 > 0, \tag{21}$$

we have

$$\begin{aligned}\bar{f} &= f_b\bar{F}_0\,\bar{cos}\,t - m_b\boldsymbol{Y}_0\ddot{\bar{\boldsymbol{\Phi}}} - m_b\boldsymbol{Y}_0\bar{\boldsymbol{\Lambda}}^2\bar{\boldsymbol{\Phi}} \\ &= f_b\bar{F}_0\,\bar{cos}\,t - m_b\ddot{\bar{y}} - k_b(\bar{\boldsymbol{\Phi}})\bar{y},\end{aligned} \tag{22}$$

where

$$\begin{aligned}k_b(\bar{\boldsymbol{\Phi}}) = m_b\frac{\boldsymbol{Y}_0\bar{\boldsymbol{\Lambda}}^2\bar{\boldsymbol{\Phi}}}{\boldsymbol{Y}_0\bar{\boldsymbol{\Phi}}} &= \frac{m_b\sum_{n=1}^{N}Y_{n0}\bar{\bar{\Omega}}_n^2\bar{\varphi}_n}{\sum_{n=1}^{N}Y_{n0}\bar{\varphi}_n}, f_b \\ &= m_b\boldsymbol{Y}_0\bar{\boldsymbol{m}}^{-1}\boldsymbol{Y}_F^T.\end{aligned} \tag{23}$$

Substituting Equation (22) into Equation (14), we obtain

$$\begin{aligned}(\bar{\boldsymbol{M}} + \boldsymbol{m}_b)\ddot{\boldsymbol{q}} + 2[\bar{\boldsymbol{M}}\bar{\boldsymbol{\omega}}\boldsymbol{E} + \boldsymbol{\varepsilon}(\boldsymbol{q})]\dot{\boldsymbol{q}} \\ + \{\boldsymbol{k}_b + [\bar{\boldsymbol{M}}\bar{\boldsymbol{\omega}}^2 + \boldsymbol{k}(\boldsymbol{q}) + \boldsymbol{k}_1(\boldsymbol{q})]\}\boldsymbol{q} = \boldsymbol{f}_b,\end{aligned} \tag{24}$$

$\boldsymbol{m}_b = \text{diag}(0,m_b), \quad \boldsymbol{k}_b = \text{diag}(0,k_b), \quad \boldsymbol{f}_b = [0 \quad f_b]^T\bar{F}_0\,\bar{cos}\,t.$

Here, m_b, k_b represent an additional dynamic mass and stiffness, respectively, which are added to the nonlinear suspension system by the beam due to their

dynamic interactions. f_b defines a force factor at which the excitation force is added to the lumped mass. The values of these added parameters depend on the retained mode number of the beam. The added stiffness k_b also involves the dynamic response $\bar{\boldsymbol{\Phi}}$ of the beam. For a unit dynamic response of mode n, i.e. $\bar{\boldsymbol{\Phi}}^T = [0 \quad \cdots \quad 0 \quad \bar{\varphi}_n \quad 0 \quad \cdots \quad 0]^T$, the added mass and stiffness are respectively obtained by Equation (25) and (26)

$$m_b = \bar{M}_{nn} Y_{n0}^{-2}, \tag{25}$$

$$k_b(\bar{\varphi}_n) = m_b \bar{\hat{\Omega}}_n^2 = \bar{M}_{nn} Y_{n0}^{-2} \bar{K}_{nn} / \bar{M}_{nn} = Y_{n0}^{-2} \bar{K}_{nn}. \tag{26}$$

Figure 2(a) shows that the additional dynamic mass, $\bar{m}_b$ decreases as the number of retained mode N increases. Each mode has a natural frequency associated with it. The natural frequency of the structure depends on the mass and stiffness distributions in the structure. The equation of natural frequency is

$$\hat{\Omega}_n = \sqrt{\frac{K_{nn}}{M_{nn}}} \tag{27}$$

As the natural frequency increases, the mass decreases and vice versa. The value of force factor at which the excitation force is added to the lumped mass greatly depends on the point, ξ_0, at which the excitation force is applied to on the beam. From Figure 2(b), at ξ_0 = 1, the force factor is a positive value at odd numbers of retained modes and negative at even numbers of retained modes. The positive value defines a pulling force while the negative value implies a compressed force. Figure 2(c) and Figure 2(d) show graphs of dynamic response of mode n for the added mass and stiffness. From Figure 2(c), it can be seen that the additional mass, m_b (φ_n) decreases as the mode number increases. However, the value of additional mass for mode numbers n = 3, 4, and 5 continue to have a similar value which is approximately 0.5. From Figure 2(d), it can be seen that the additional dynamic stiffness, k_b (φ_n) added to the nonlinear suspension system by the beam increases as the mode number increases. The increase in additional stiffness is very large from 67 at n = 2 to 30787 at n = 5. Referring to Equation (27), increase in mode number means increase in the natural frequency, thus increase in the stiffness of the structure.

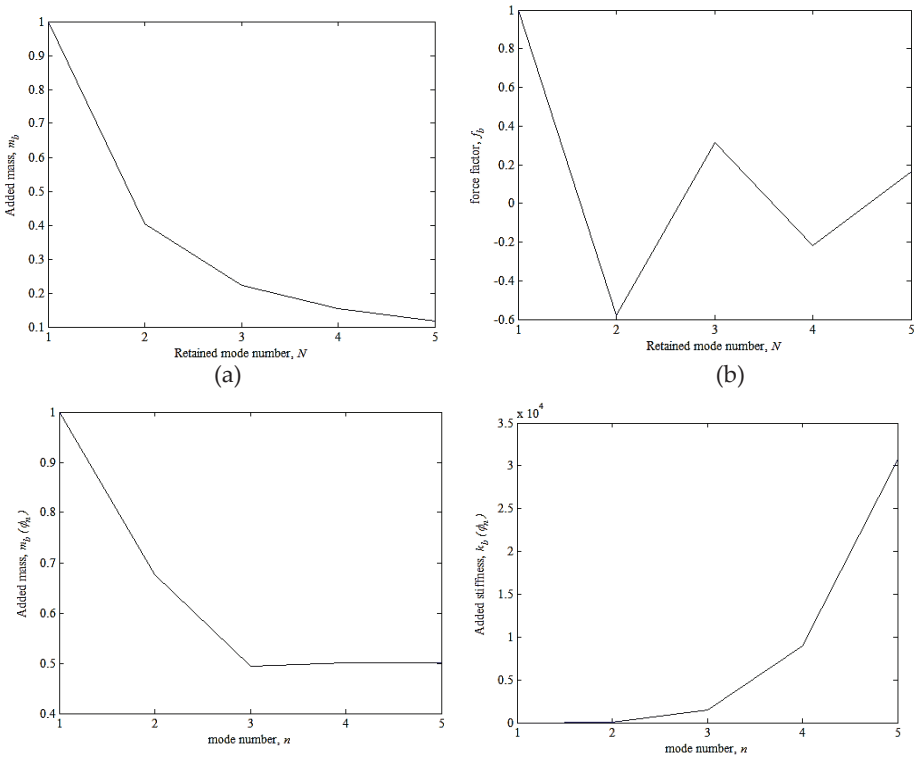

Figure 2 (a) Graph of additional mass $\bar{m}_b$ with respect to retained mode number, (b) Graph of force factor with respect to retained mode number, (c) Graph of added mass for a unit dynamic response with respect to mode number, (d) Graph of added stiffness for a unit dynamic response with respect to mode number

The two components of stiffness forces are

$$\boldsymbol{F}_R = \{\boldsymbol{k}_b + [\bar{\boldsymbol{M}}\bar{\boldsymbol{\omega}}^2 + \boldsymbol{k}(\boldsymbol{q}) + \boldsymbol{k}_1(\boldsymbol{q})]\}\boldsymbol{q} \tag{28}$$

of which the horizontal component is not affected by the beam motion while the vertical component is affected by the additional added stiffness of the beam onto the nonlinear supporting unit. We choose the static position $\boldsymbol{q}_0 = [q_{10}\ 0]^T$ satisfying Equation (1) as a zero point of the potential energy, that is

$$\Pi[\boldsymbol{q}_0] = \bar{m}\bar{\omega}^2 q_{10}^2 - \bar{k}q_{10} - \bar{f}_1 q_{10} = 0 \tag{29}$$

The potential energy at position **q** of the system is

$$\begin{aligned}\Pi[\boldsymbol{q}] &= \int_{\boldsymbol{q}_0}^{\boldsymbol{q}} d\boldsymbol{q}^T \\ &= \left[\frac{1}{2}\boldsymbol{q}^T(\boldsymbol{k}_b + \bar{\boldsymbol{M}}\bar{\boldsymbol{\omega}}^2)\boldsymbol{q}\right]_{\boldsymbol{q}_0}^{\boldsymbol{q}} - \frac{1}{2}\int_{\boldsymbol{q}_0}^{\boldsymbol{q}} \bar{k}(\boldsymbol{q}^T\boldsymbol{q})^{-\frac{1}{2}} d(\boldsymbol{q}^T\boldsymbol{q}\Big) \\ &- \bar{f}_1(q_1 - q_{10}) \\ &= \frac{1}{2}[\bar{m}\bar{\omega}^2(q_1^2 - q_{10}^2) + \bar{\Omega}^2 q_2^2 + k_b q_2^2] - \bar{k}(\boldsymbol{q}^T\boldsymbol{q})^{1/2} + \bar{k}q_{10} \\ &- \bar{f}_1 q_1 + \bar{f}_1 q_{10} \\ &= \frac{1}{2}[\bar{m}\bar{\omega}^2(q_1^2 + q_{10}^2) + \bar{\Omega}^2 q_2^2 + k_b q_2^2] - \bar{k}\sqrt{q_1^2 + q_2^2} \\ &- \bar{f}_1 q_1.\end{aligned} \tag{30}$$

In this equation, the term $k_b q_2^2/2$ represents the elastic energy of the beam, which vanishes if only the beam rigid mode is retained.

The graph in Figure 3 (a) show the horizontal component of stiffness force for different values of k_b. Figure 3 (b) until (f) show the vertical component of stiffness force affected by different values of k_b.

From Equation (28) the horizontal stiffness force F_{R1} and the vertical stiffness force F_{R2} of the beam and nonlinear suspension unit can be derived. From here, the parameters that affect the stiffness forces can be identified.

Inserting the values of $\boldsymbol{k}_b$,$\bar{\boldsymbol{M}}$, $\bar{\boldsymbol{\omega}}^2$, $\boldsymbol{k}(\boldsymbol{q})$, $\boldsymbol{k}_1(\boldsymbol{q})$ and $\boldsymbol{q}$ from Equation (15) and (24) we obtain

$$\begin{aligned}\boldsymbol{F}_R = \Bigg[\boldsymbol{k}_b + \Bigg(\begin{bmatrix}\bar{m} & 0\\ 0 & 1\end{bmatrix}\begin{bmatrix}\bar{\omega}^2 & 0\\ 0 & \bar{\Omega}^2\end{bmatrix} + -\frac{\bar{k}}{\bar{\mu}}\boldsymbol{I} \\ + -\frac{\bar{f}_1}{q_1}\boldsymbol{I}_1\Bigg)\Bigg]\begin{bmatrix}q_1\\ q_2\end{bmatrix}\end{aligned} \tag{31}$$

$$\begin{bmatrix}F_{R1}\\ F_{R2}\end{bmatrix} = \begin{bmatrix}\left(\bar{m}\bar{\omega}^2 - \dfrac{\bar{k}}{\sqrt{q_1^2 + q_2^2}} - \dfrac{\bar{f}_1}{q_1}\right)q_1 \\ \left(k_b + \bar{\Omega}^2 - \dfrac{\bar{k}}{\sqrt{q_1^2 + q_2^2}}\right)q_2\end{bmatrix}$$

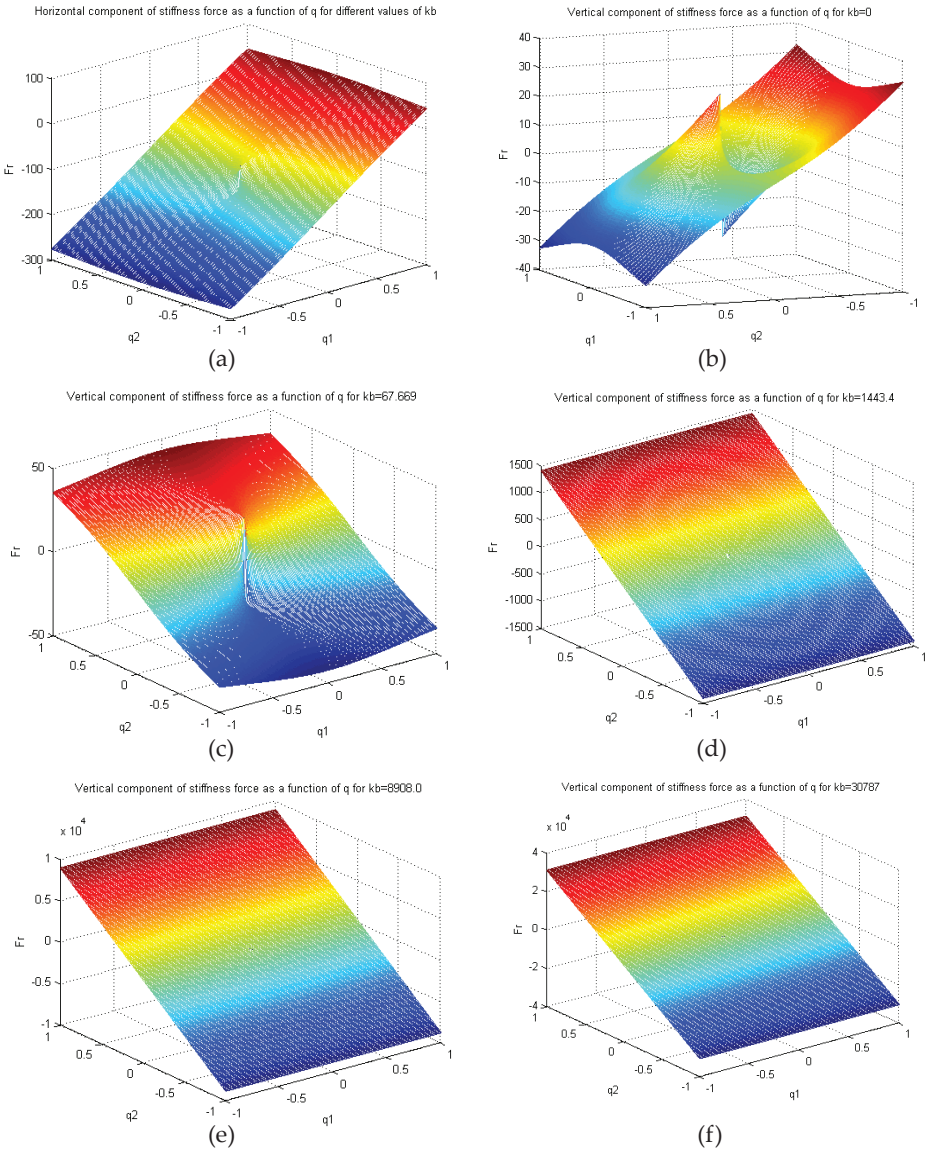

Figure 3 (a) Horizontal nonlinear stiffness force affected by kb, (b) Vertical nonlinear stiffness force when kb = 0, (c) Vertical nonlinear stiffness force when kb = 67.99, (d) Vertical nonlinear stiffness force when kb = 1443.4, (e) Vertical nonlinear stiffness force when kb = 8908, (f) Vertical nonlinear stiffness force when kb = 30787

It can be seen in Figure 3(a) that the value of k_b does not affect the horizontal component of stiffness force. The graphs overlap each other even though different values of k_b are used. This is also proven from Equation (31), whereby there is no k_b term in the equation for the horizontal stiffness force F_{r2}.

In Figure 3 (b) to Figure 3 (f), the values of k_b is seen to affect the vertical stiffness force. When the value of k_b = 0 and k_b = 67.99, the graphs illustrate a nonlinear behaviour, but for larger values of k_b, the graph becomes a linear graph. This is because, larger values of k_b result in k_b being dominant over all the other terms (including the nonlinear term) in the vertical stiffness force equation.

There is a potential energy associated with the stiffness force, which can be found by integrating the force with displacement. The potential energy at position **q** of the system is given by Equation (30). Figure 4 (a) to Figure 4 (e) show the potential energy at position **q** (static equilibrium position) of the system with different values of k_b.

When k_b is zero, which means there is no elastic energy in the beam, and the beam is in its rigid mode, the graph of potential energy varies across q_1 (x-axis). When there is a value of k_b the graph varies across q_2 (y-axis). This is in line with the equation of stiffness forces whereby k_b only affects the y-axis. As k_b increases, so does the value of potential energy.

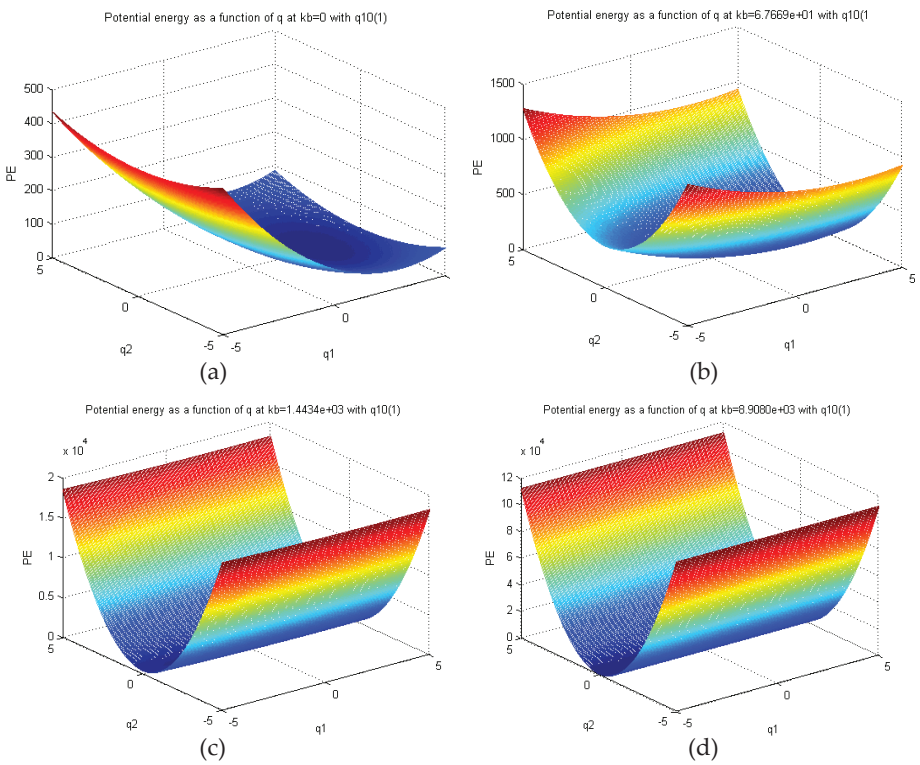

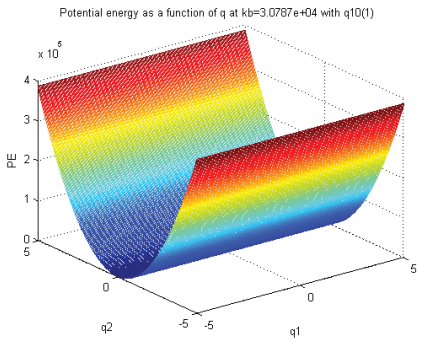

(e)

Figure 4 Potential energy for position q at the static position q_{10} = 0.6471 at (a) k_b = 0, (b) k_b = 67.99, (c) k_b = 1443.4, (d) k_b = 8908 and (e) k_b = 30787

3.0 BEAM-NONLINEAR ISOLATOR DESIGN

3.1 Low Stiffness Support

We consider Figure 1 as a simplified model for ground vibration tests of large full-scale aircrafts. The central mass is considered as the mass of the fuselage and the two beams connected to the central mass are the two wings of the aircraft. Aircrafts flying in the air are in a free-free state without any mechanical supports. However, in tests, the aircraft is supported on the ground so the supporting system will have an affect on the aircraft's dynamic characteristics. For a reliable test result, the effect of supporting system should be as less as possible. It has been demonstrated that the effect of supporting system on the aircraft could be neglected if the frequency of an assumed rigid aircraft Ω_{SA}, on the supporting system is less than one third of the first elastic natural frequency of the free-free aircraft Ω_{EA} (Molyneux 1958; Xing 1975), i.e.

$$\Omega_{SA} \leq \Omega_{EA}/3 \tag{32}$$

For small aircrafts, their first elastic natural frequency is high enough and there is no difficulty to design a supporting system satisfying Equation (19). However, for very large aircrafts, the first natural frequency, usually the first-order bending frequency of aircraft wings is lower than 1 Hz. Therefore, the supporting frequency for large aircraft tests should be less than 0.3 Hz. Due to a very large weight of the aircraft supported in the static state, the static stiffness of the supporting system must be sufficiently large to balance the

heavy weight. As a result, it is very difficult to design a supporting system with less than 0.3 Hz supporting frequency for large aircrafts by means of normal supporting designs, such as air spring system etc. (Molyneux 1958; Xing 1975). Nonlinear supporting system provides an effective approach to design this type of supporting systems.

To support the airplane on the ground, a point is chosen as the static equilibrium state of the aircraft on the ground. Based on Equation (1), $\Delta = Y_0 - L$, from which we can choose a suitable height Y_0 according to the initial length L of the vertical spring, so that a negative parameter $\bar{\Delta}$ and the vertical stiffness $\bar{K}$ are determined by

$$\bar{K} = (1 + \bar{\rho}\bar{S})\bar{g}/|\bar{\Delta}|, \qquad K = M\Omega_0^2\bar{K} \tag{33}$$

Because the total mass of the large airplane is huge, the stiffness of the vertical spring is very large. If there are no two inclined springs, the supporting frequency of the aircraft and the static compression of the vertical spring are required to satisfy the conditions

$$\Omega_{SA} = \sqrt{\bar{K}/(1 + \bar{\rho}\bar{S})} = \sqrt{\bar{g}/|\bar{\Delta}|} \leq \Omega_{EA}/3, \qquad |\bar{\Delta}| \geq 9\bar{g}/\Omega_{EA}^2 \tag{34}$$

A limited space of test site does not allow these conditions to be realised only using linear supporting systems. The natural frequency is found to be

$$\Omega_{NSA} = \hat{\bar{\Omega}}_2^{(1)} = \sqrt{(1 - \bar{k}\bar{\Omega}^{-2}/\bar{\mu}_0^{(1)})/(1 + \tilde{\rho}\tilde{S})}\bar{\Omega}, \bar{\mu}_0^{(1)} = \tilde{k}_1 + \tilde{K}_1\bar{\Delta}_1 \tag{35}$$

Based on Equations (8) and (12), we obtain

$$\bar{\Delta}_1 = (X_0 - L_1)/l, \qquad \bar{\mu}_0^{(1)} = \tilde{K}_1(k/K_1 + \bar{\Delta}_1), \tag{36}$$

so that to reduce the supporting frequency Equation (35) we must choose a point to design the system satisfying

$$1 \geq \bar{k}\bar{\Omega}^{-2}/\bar{\mu}_0^{(1)} > 0, \qquad \tilde{k}_1 + \tilde{K}_1\bar{\Delta}_1 > 0 \tag{37}$$

This design condition is easily realised. In this design, the nonlinear stiffness term $\bar{k}\bar{\Omega}^{-2}/\bar{\mu}_0^{(1)}$ plays a negative stiffness in Equation (35) to reduce the supporting frequency. Theoretically, from Equation (37), we may choose the value of $\bar{k}\bar{\Omega}^{-2}/\bar{\mu}_0^{(1)}$ near to 1 to realise the standard $\Omega_{NSA} < \Omega_{EA}/3$.

3.1.1 Choosing suitable parameters

The suitable parameters are first chosen to satisfy Equation (37). The values of stiffness K and K_1 can be found from Equation (1). The value of stiffness k is chosen to be the same as K.

$$\begin{aligned} K &= \frac{-g(M+\rho s)}{\Delta}, & \Delta &= Y_0 - L \\ K_1 &= \frac{k(l-x_0)}{x_0 - \Delta_1}, & \Delta_1 &= X_0 - L_1 \end{aligned} \tag{38}$$

3.1.2 Linear analysis

Linear analysis is done by applying small vibration about the chosen equilibrium point to find the natural frequencies and modes of the system which will be compared with the natural frequencies and modes of the free-free beam. Using the eigenvalue equation, the eigenvalues and eigenvectors of the beam affected by the nonlinear isolator are found. The eigenvalues are the natural frequencies of the beam supported on the nonlinear isolator and is shown in Table 1. The eigenvectors are the generalised coordinates which is used to find the mode shapes of the beam supported on the nonlinear isolator. Using the mode summation equation in (3), the normalised mode shapes are found as shown in Figure 5. The natural frequencies and modes of the free-free beam are shown in Table 2 and Figure 6. By comparing Table 1 with Table 2, the natural frequencies at the chosen equilibrium point are a little lower than the corresponding one of the free - free beam. This is caused by the lumped mass M of the supporting isolator which does not exist in the free - free beam. At N=1 (rigid mode in the vertical direction), the natural frequency of the beam supported on the nonlinear support is 6.7435e-7 which is less than one third of the first elastic natural frequency (N=2) of the free-free beam. This satisfies the requirement of Equation (37).

Table 1 Natural frequencies of beam supported on the nonlinear support at the chosen equilibrium point

n	1	2	3	4	5
Frequency	6.7435e-7	1	5.3902	13.3146	24.7658

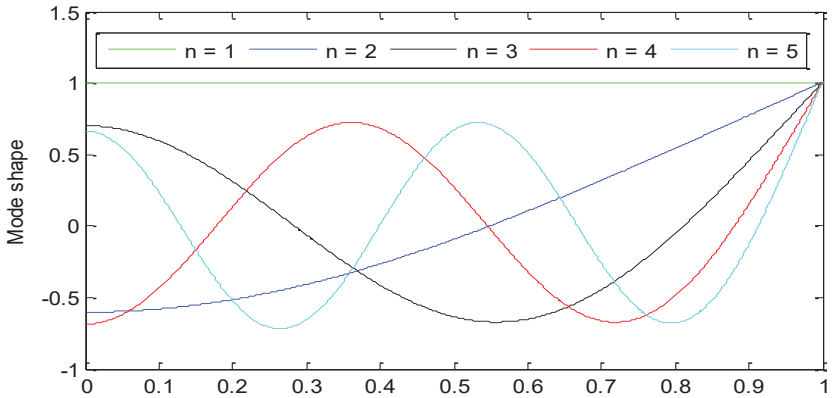

Figure 5 Mode shapes of the beam affected by the nonlinear isolator for mode, *n*=1 to 5

Table 2 Natural frequency of the free-free beam

N	1	2	3	4	5
Frequency	0	1	5.4039	13.3443	24.8139

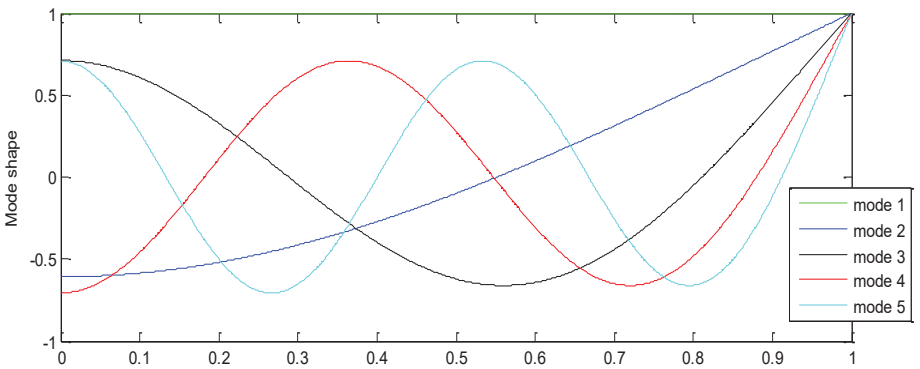

Figure 6 Mode shapes of the free-free beam

The mode shapes of the beam supported on the nonlinear isolator in Figure 5 are compared to the mode shapes of the free free beam in Figure 6, and it can be seen that the mode shapes of the beam on the nonlinear isolator is similar to mode shapes of the free free beam.

3.1.3 Dynamic response

The dynamic response of the system is analysed by applying two sinusoidal excitation force to the beam. Equation (18) of the integrated coupling equation of the system in state space form was inserted into the Simulink Differential Equation Editor block and the parameters in Matlab m-file was defined. Because the system is a nonlinear system, it will exhibit nonlinear behaviour, thus chaos and bifurcation will be studied. To observe the nonlinear dynamical behaviour of bifurcation and chaos, the phase plane plot of velocity vs displacement for the vertical motion of the beam at n=1 is shown in Figure 7 (a) to (e).

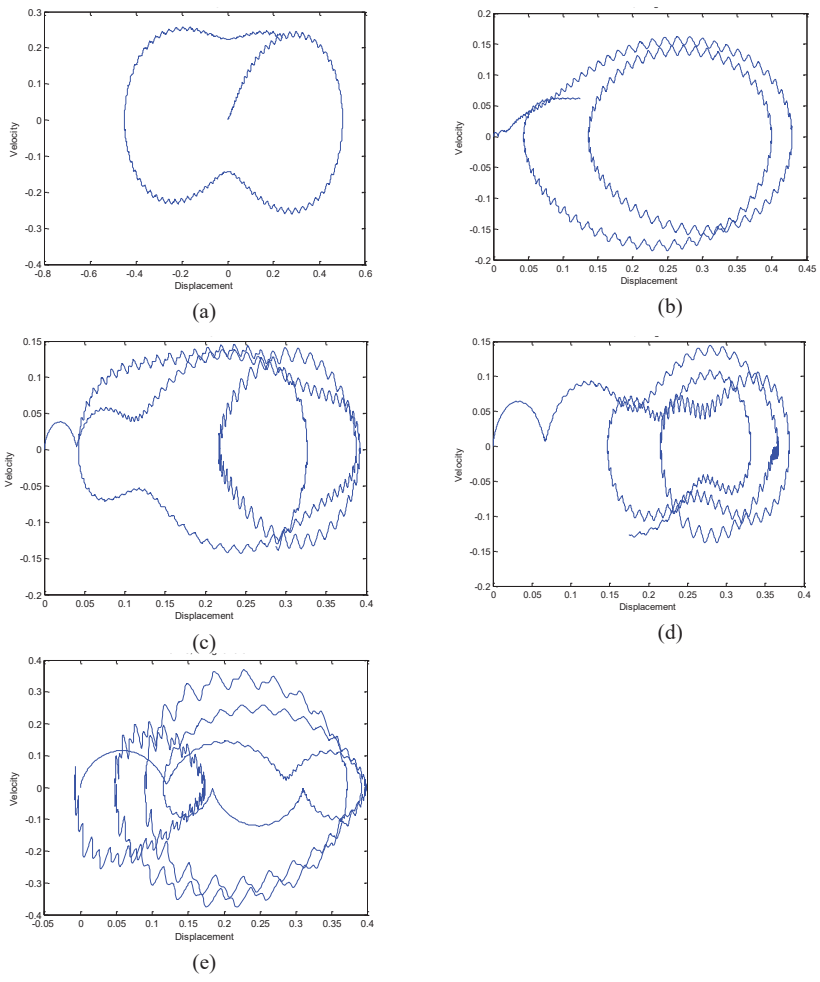

Figure 7 (a) Phase plane plot when $F_0 = 0.01$, $\Omega_0 = 0.5$, (b) Phase plane plot when $F_0 = 1$, $\Omega_0 = 0.5$, (c) Phase plane plot when $F_0 = 6$, $\Omega_0 = 0.5$, (d) Phase plane plot when $F_0 = 12$, $\Omega_0 = 0.5$, (e) Phase plane plot when $F_0 = 18$, $\Omega_0 = 0.5$

Fixing the value of excitation frequency Ω_0 = 0.5, F_0 is varied to observe the condition for bifurcation and chaos. From Figure 7 (a), when F_0 = 0.01, the response is a 1 period motion. When F_0 = 1, period doubling bifurcation starts to happen as shown in Figure 7 (b). When F_0 = 6 and F_0 = 12 a 4 period motion can be observed as shown in Figure 7 (c) and (d). Increasing the value of excitation force to F_0 = 18, a 8 period motion is observed in Figure 7 (e).

Increasing the excitation force F_0 = 20 and varying the excitation frequency Ω_0 from 0.1Hz to 100Hz, Poincare' maps where plotted in Figure 8 to observe the behaviour of the system. It can be seen that the Poincare' maps all form closed loops and no chaotic orbit is observed.

3.2 High Stiffness Support

The system shown in Figure 1 is considered as a model of laboratory dynamic tests. In this test, a beam that is to be tested is symmetrically fixed at a platform of mass supported by the nonlinear isolation unit. The beam is intended to be fixed on the "rigid" foundation. This implies that the supported unit should have an extremely large supporting stiffness and frequency.

The supporting frequency given in Equation (35) is still valid. From Equation (36), to obtain an extremely high frequency, it is necessary to choose an equilibrium point in the left half part of the symmetrical system satisfying

$$\bar{k}\bar{\Omega}^{-2}/\bar{\mu}_0^{(1)} < 0, \qquad \tilde{k}_1 + \tilde{K}_1\bar{\Delta}_1 < 0. \tag{39}$$

In this design, the nonlinear stiffness term $\bar{k}\bar{\Omega}^{-2}/\bar{\mu}_0^{(1)}$ plays a positive stiffness in Equation (35) to increase the supporting frequency. Theoretically, choosing a very small negative value of $\tilde{k}_1 + \tilde{K}_1\bar{\Delta}_1$ satisfying Equation (39), a sufficiently large supporting frequency can be obtained to treat the supporting foundation as "rigid".

The fixed –free beam is used as a theoretical model for studying the high stiffness support. The eigenvalue equation was solved numerically using Matlab and the eigenvalues and eigenfunctions of the beam supported on the nonlinear isolator for high stiffness support were found. The eigenvalues are the natural frequencies of the beam for mode n = 1 to 5 and is shown in Table 4.

At the first mode, a very high natural frequency of 3.0821e+3 has been obtained. When compared to the natural frequencies of the fixed - free beam in Table 3, it can be seen that the first frequency is much lower than the theoretical one (infinity), while the other frequencies (at mode n = 2,3,4,5) are higher than the theoretical one. The eigenfunctions are the generalised coordinates of the beam which is used in the mode summation equation in (3) to find the mode shapes of the beam supported on the nonlinear isolator as shown in Figure 10.

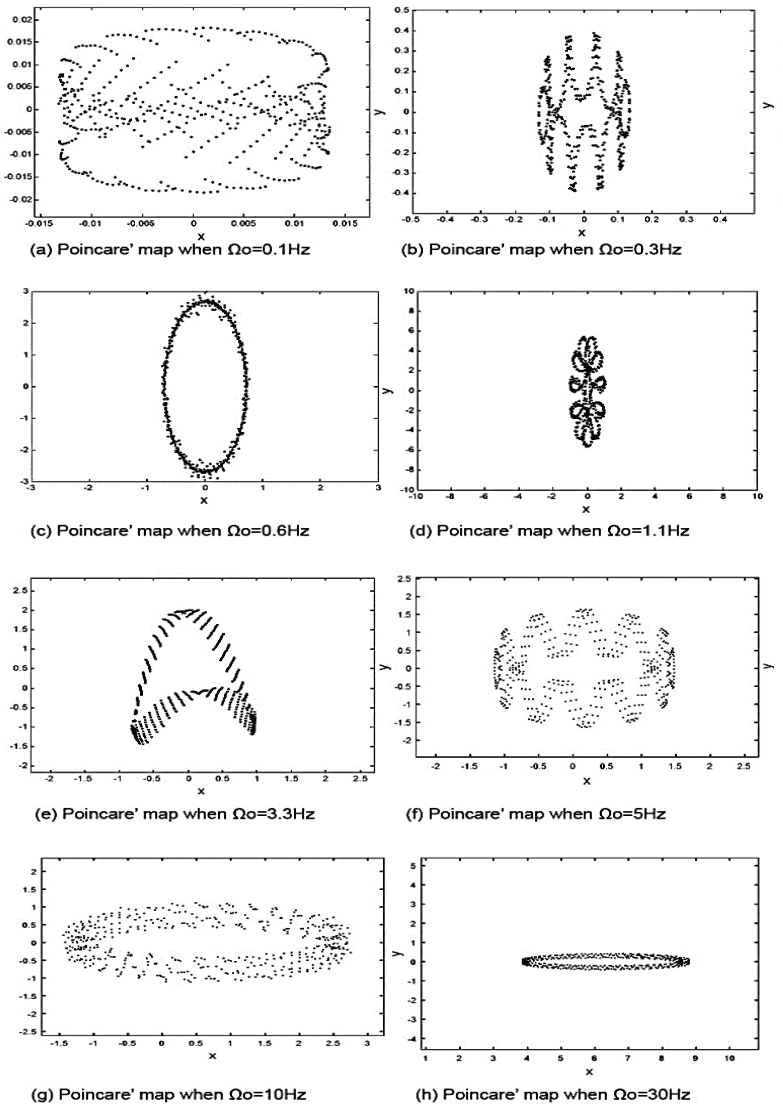

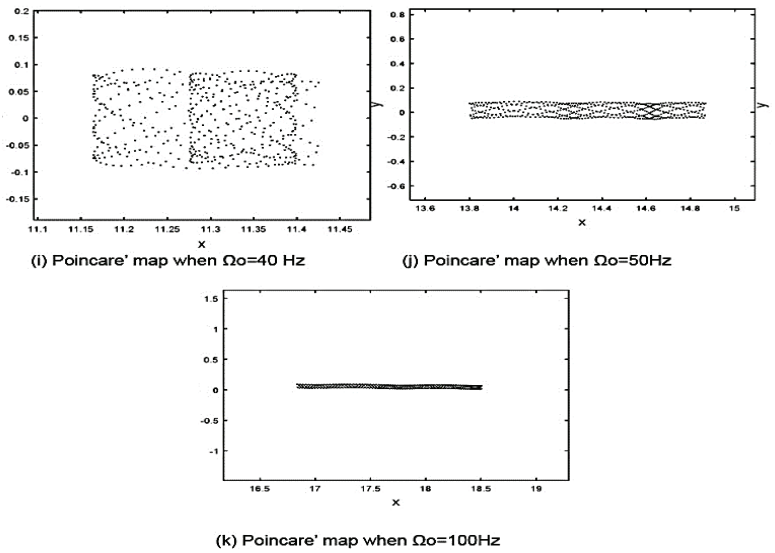

Figure 8 Poincare' maps of the system when F_0=20 and (a)Ω_0=0.1Hz, (b)Ω_0=0.3Hz, (c)Ω_0=0.6Hz, (d)Ω_0=1.1Hz, (e)Ω_0=3.3Hz, (f)Ω_0=5Hz, (g)Ω_0=10Hz, (h)Ω_0=30Hz, (i)Ω_0=40Hz, (j)Ω_0=50Hz, (k)Ω_0=100Hz

Table 3 Natural frequencies of fixed- free beam

N	1	2	3	4	5
Frequency	∞	62.854	393.9279	1.1031e+3	2.1617e+3

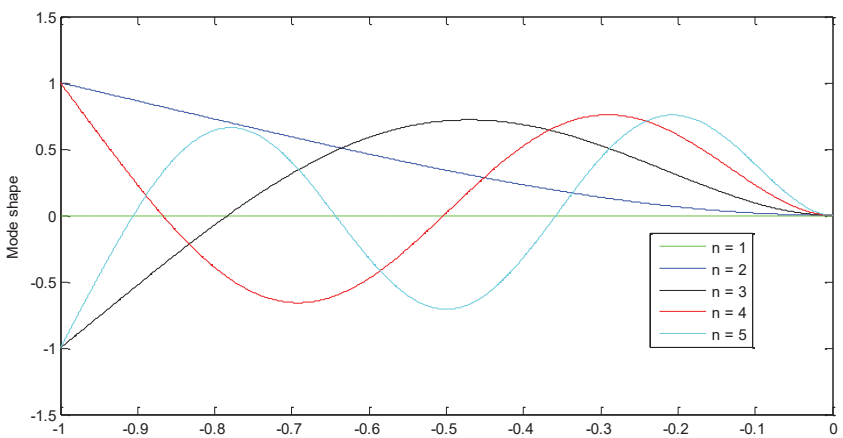

Figure 9 Mode shapes of the fixed-free beam

Table 4 Natural frequencies of beam on nonlinear vibration isolator with high stiffness support

N	1	2	3	4	5
Frequency	3.0821+3	76.9839	484.2000	1.3651e+3	2.7081e+3

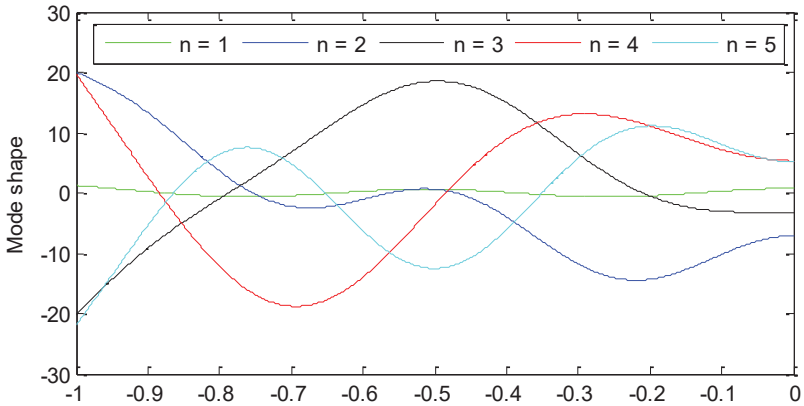

Figure 10 Mode shapes of beam on nonlinear isolator for modes *n*=1 to 5

4.0 PERFROMANCE ANALYSIS

To evaluate the performance of the nonlinear isolator, a performance analysis was done by looking at the force transmissibility of the nonlinear isolator. Transmissibility is a measure of the reduction of vibration transmitted from a source to a receiver, in other words, it is an index of the performance of an isolator (Carella, 2008). Force transmissibility is the ratio between the magnitude of transmitted force (receiver) over magnitude of excitation force (source). A harmonic excitation force is acted upon the nonlinear isolator in Equation (14). The force transmissibility was found numerically using Matlab's ode45 solver with a given excitation force of F_0=0.6, and varying the excitation frequency, Ω_0 from 0 to 100 Hz. An excitation force of F_0=0.6 was used so that the magnitude of transmissibility at 0 frequency ratio, Ω_0/Ω is 0 dB. This means that the transmitted force is the same as the excitation force at Ω_0/Ω=0. The force transmissibility of the nonlinear isolator is compared to the force transmissibility of a linear isolator as shown in Figure 11, using values of damping ratio of vertical damper, *E*=6.15e-4, stiffness of oblique spring, *k*=*K* (stiffness of vertical spring) and initial condition

y0=[0.5 0 7 0]. The initial condition is defined by y0=[q_1 $\dot{q}_1$ q_2 $\dot{q}_2$] where q_1: displacement of mass, m in the horizontal direction, $\dot{q}_1$: velocity of mass, m in the horizontal direction, q_2: displacement of mass, M in the vertical direction, $\dot{q}_2$: velocity of mass, M in the vertical direction. The initial condition used, y0=[0.5 0 7 0] means that the initial displacement of mass m is at 0.5 and the initial displacement of mass M is at 7. This also defines the position of the oblique spring. Figure 11 shows the transmissibility plot in decibel (dB) scale for the nonlinear isolator and linear isolator. The linear isolator consists of a mass with a vertical spring and damper. The effectiveness of a vibration isolator can be measured by looking at the bandwidth of the isolation region and peak transmissibility (Carella, 2008). Isolation region is the frequency region within which the transmitted force becomes smaller than the excitation force, that is when the transmissibility is less than 1, or 0 dB. Peak transmissibility is the maximum amplitude of the transmitted force for a given amplitude of input force. It can be seen from Figure 11 that the transmissibility of the nonlinear isolator has a wider isolation region and a lower peak transmissibility compared to the linear isolator. This shows that the nonlinear isolator performs better than a linear isolator.

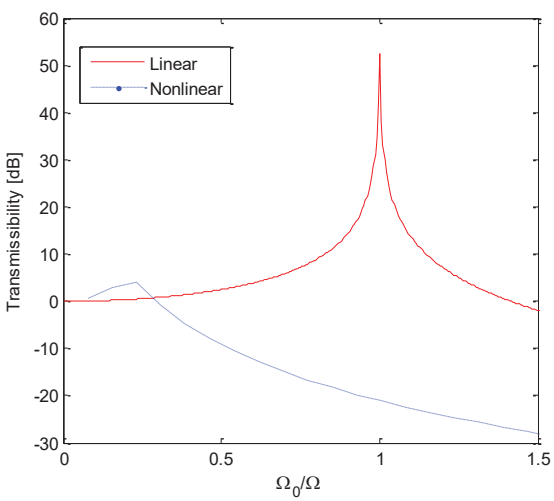

Figure 11 Force transmissibility of nonlinear isolator compared to a linear isolator

To observe the effect of changing the position of the oblique spring, the initial condition y0 was varied and the force transmissibility of the nonlinear isolator is shown in Figure 12 (a). It is shown that the isolation region is wider as the initial

displacement of the mass in the vertical direction is increased. Therefore, it is better to have a higher value of initial displacement of the mass in the vertical direction. Figure 12 (b) shows the force transmissibility of the nonlinear isolator when the damping coefficient is varied. It can be seen that the peak transmissibility decreases as the damping coefficient increases. A reasonable amount of damping can therefore decrease the peak transmissibility which is beneficial for the performance of the nonlinear isolator. The force transmissibility of the nonlinear isolator with varying stiffness of the oblique spring is shown in Figure 12 (c). It can be observed that as the stiffness increases, the beginning value of transmissibility increases and peak transmissibility also increases. Therefore, it is advised that a lower stiffness of the vertical spring is to be used to obtain a better performance for the nonlinear isolator. Finally, the force transmissibility of the nonlinear isolator is compared to the force transmissibility of a hardening HSLDS mount (Carella, 2008) as shown in Figure 12 (d). It can be seen that the nonlinear isolator has a lower peak transmissibility and a wider isolation region and therefore has a better performance compared to the HSLDS mount.

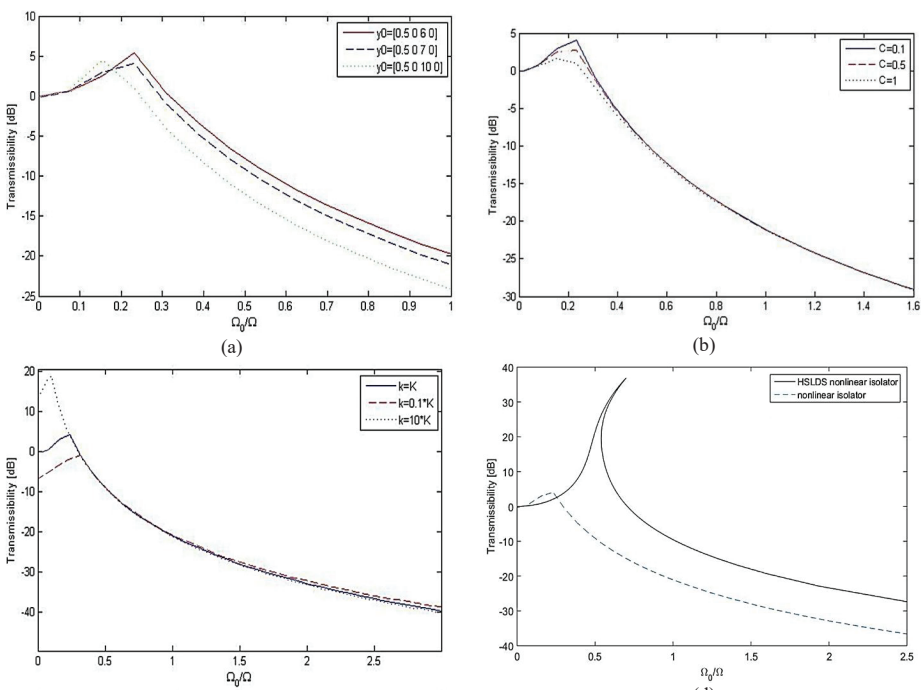

Figure 12 (a) Force transmissibility of nonlinear isolator with different initial conditions, (b) Force transmissibility of nonlinear isolator with varying damping coefficients, (c) Force transmissibility of nonlinear isolator with varying stiffness, (d) Force transmissibility of nonlinear isolator compared with HSLDS isolator

5.0 CONCLUSION

The beam is found to provide additional mass, stiffness and force to the nonlinear isolator. The design for low frequency support shows that the natural frequencies and mode shapes of the beam supported by the nonlinear isolator at modes n=1 to n=5 was found to be similar to the free-free beam natural frequencies and mode shapes. The frequency obtained at n=1 (rigid mode) of the beam is 6.7435e-7 which is less than one third of the first elastic natural frequency (n=2) of the free-free beam which has a value of 1. This satisfies the requirement to perform ground vibration test. Nonlinear behaviour of period doubling bifurcation is seen to occur when F_0=1 and Ω_0=0.5Hz. Poincare' maps showed closed loop and no chaos was observed. The force transmissibility of the nonlinear isolator indicates that it can perform better than a linear isolator and also performs better than a HSLDS mount.

ACKNOWLEDGEMENTS

The authors are grateful to Faculty of Engineering and Physical Science, University of Southampton, United Kingdom for the technical support provided for the research work.

REFERENCES

Cao, Q., Wiercigroch, M., Pavlovskaia, E. E., Grebogi, C., & Thompson, J. M. T. (2008a). The limit case response of the archetypal oscillator for smooth and discontinuous dynamics. *International Journal of Non-Linear Mechanics*, 43(6), 462–473.

Cao, Q., Wiercigroch, M., Pavlovskaia, E. E., Thompson, J. M. T., & Grebogi, C. (2008b). Piecewise linear approach to an archetypal oscillator for smooth and discontinuous dynamics. *Philosophical Transactions. Series A, Mathematical, Physical, and Engineering Sciences*, 366(1865), 635–652.

Carrella, A. (2008). *Passive vibration isolators with high-static-low-dynamic-stiffness*. (Doctoral thesis). University of Southampton. Retrieved from http://eprints.soton.ac.uk/id/eprint/51276

Green, G. S. (1945). The effect of flexible ground supports on the pitching vibrations of an aircraft. *R&M*, 2291.

Inman, D. J. (2007). *Engineering Vibration* (Third.). Prentice Hall.

Kovacic, I., Brennan, M. J., & Waters, T. P. (2008). A study of a nonlinear vibration isolator with a quasi-zero stiffness characteristic. *Journal of Sound and Vibration*, 315(3), 700–711.

Liu Yan-bin, Yu-shu, C., & Qing-jie, C. (2012). Bifurcations of resonance in an irrational system. *Vibration and Shock*, 31, 151–154.

Molyneux, W. G. (1958). The Support of an Aircraft for Ground Resonance Tests. *Aircraft Engineering and Aerospace Technology*, 30(6), 160–166.

Platus, D. L. (1992). *Negative-stiffness-mechanism vibration isolation systems*. Proc. SPIE 1619, Vibration Control in Microelectronics, Optics, and Metrology

Rivin, E. (2003). *Passive Vibration Isolation*. ASME Press.

Thomson, W. (1996). *Theory of Vibration with Applications*. CRC Press.

Wagg, D., & Nield, S. (2010). *Nonlinear Vibration with Control*. Springer.

Xing, J. T., Xiong, Y. P., Djidjeli, K., & Turahim, K. K. (2017) A Generalised Nonlinear Isolator-Elastic Beam Interaction Analysis for Extremely Low or High Supporting Frequency. At *9th European Nonlinear Dynamics Conference (ENOC 2017), Hungary*. 10 pp.

Xing, J.-T., & Price, W. G. (1991). *A mixed finite element method for the dynamic analysis of coupled fluid-solid interaction problems*. Proceedings of the Royal Society: Mathematical and Physical Science.

Xing, J. T. (1975). Theory and techniques on mode vibration experiments of aircraft structures. *In Theory and techniques on mode vibration experiments of aircraft structures*. NAI press.